EFFECT of SYNTHESIS PARAMETERS on the CRYSTAL STRUCTURE of $La_{1-x}Ca_xMn_yAl_{1-y}$ (LCMA)

Berke PİŞKİN*, Department of Metallurgical and Materials Engineering, Faculty of Engineering, Mugla Sitki Kocman University, Turkey

berkepiskin@mu.edu.tr(https://orcid.org/0000-0001-8372-5039)

Abstract

Hydrogen is an essential substance for green-energy applications. The production of hydrogen-based on renewable energy sources has a critical role in this context. Thermochemical methods based on solar energy are getting attention for hydrogen production in a sustainable manner. It is possible to produce hydrogen without the need of purification via two-step thermochemical water splitting (TWS) method. The thermodynamics and kinetics of redox reactions in active materials used are the important factors for determining the hydrogen production efficiency. The structural stability is another concern in the TWS reactions. The efficiency is strongly influenced by the structural properties of active materials used in these reactions. In this regard, perovskite-oxides draw attention as an active material that can be used in TWS reactions due to their superior structural stability together with their compositional diversity. In this study, it was aimed to investigate the effect of synthesis parameters on the structural properties of $La_{0.4}Ca_{0.6}Mn_{0.6}Al_{0.4}O_3$ (LCMA4664) and $La_{0.2}Ca_{0.8}Mn_{0.8}Al_{0.2}O_3$ (LCMA2882) perovskite-type oxides that offer high hydrogen production efficiency by TWS. It was found that different stoichiometry in LCMA oxide family has an effect on the resulting crystal structure together with the synthesis parameters.

Keywords: Perovskite oxide, Pechini Method, Thermochemical water splitting.

SENTEZ PARAMETRELERİNİN $La_{1-x}Ca_xMn_yAl_{1-y}$ (LCMA) KRİSTAL YAPISINA ETKİSİ

Özet

Yeşil enerji uygulamaları için hidrojen çok önemli bir yere sahiptir. Yenilenebilir enerji kaynaklarına dayalı hidrojen üretimi bu bağlamda kritik bir role sahiptir. Güneş enerjisine dayalı termokimyasal yöntemler, sürdürülebilir bir şekilde hidrojen üretimi için dikkat çekmektedir. İki aşamalı termokimyasal su ayırma (TSA) yöntemi ile saflaştırmaya gerek kalmadan hidrojen üretmek mümkündür. Redoks reaksiyonlarının termodinamiği ve kinetiği, hidrojen üretim verimini belirleyen önemli faktörlerden biridir ve yapısal kararlılık TSA redoks reaksiyonları için çok önemlidir. Hidrojen üretim verimliliği, redoks reaksiyonlarda kullanılan aktif malzemelerin yapısal özelliklerinden önemli bir şekilde etkilenmektedir. Bu bakımdan perovskit oksitler, kompozisyon çeşitliliği ile birlikte üstün yapısal kararlılıkları nedeniyle TWS reaksiyonlarında kullanılabilen aktif bir malzeme olarak dikkat çekmektedir. Bu çalışmada sentez parametrelerinin TWS ile yüksek hidrojen üretebilme kapasitesine sahip olan $La_{0.4}Ca_{0.6}Mn_{0.6}Al_{0.4}O_3$ (LCMA4664) ve $La_{0.2}Ca_{0.8}Mn_{0.8}Al_{0.2}O_3$ (LCMA2882) perovskit tipi oksitlerin yapısal özellikleri üzerine etkisinin araştırılması amaçlanmıştır. LCMA oksit ailesindeki farklı stokiyometrinin sentez parametreleri ile birlikte ortaya çıkan kristal yapı üzerinde etkisi olduğu bulunmuştur.

Anahtar Kelimeler: perovksit oksit, Pechini yöntemi, termokimyasal su ayrıştırma

1. Introduction

Hydrogen is an important clean energy carrier as in the case of the usage of hydrogen to generate electricity in a fuel cell where it only releases water and heat [1], [2].

Besides the usage of hydrogen in the fertilizer industry, petrochemical industry, vegetable, and animal oil production, there are many investments in the world for many applications, especially in the field of transportation, depending on hydrogen as a clean fuel [3]. With the development of these technologies, the

need for high purity hydrogen will undoubtedly increase.

A major problem to use hydrogen-based applications with their full potential is the cost of producing fuel cells and hydrogen. Since hydrogen can always be produced with different gas components such as CO, CO_2, O_2, H_2O, H_2S and NO_x, regardless of its method/source, the hydrogen produced must always undergo a purification process which is costly [4]. The development of methods by which hydrogen can be produced in a pure form with a single step that will eliminate the dependence on purification processes. This proposed project focuses on thermochemical methods that allow pure hydrogen to be produced in a single step.
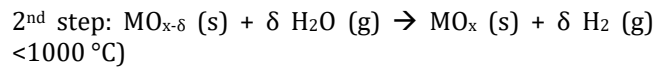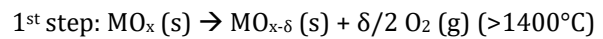
Although hydrogen is called clean energy, it depends on fossil fuels (oil, coal, and natural gas) depending on the production sources. Currently, the most economical production method is natural gas reforming [5]. With this fossil fuel-based production method, existing hydrogen production itself causes a serious amount of greenhouse gas emissions and leads to many environmental problems. Therefore, solar energy-based production methods, which is one of the production of hydrogen from renewable resources, take attention due to their efficiency and sustainability [6].

Solar hydrogen production methods are divided into two as photocatalytic and thermochemical. Photocatalytic methods can produce H_2/O_2 gas mixtures which require additional purification processes. Solar energy-based thermochemical methods, on the other hand, provide hydrogen production by decomposing water. For this reason, it is a sustainable method and provides the production of hydrogen from water (H_2O), one of the most abundant raw materials in the world [7]. Besides, in the separation of water, unlike the other process, solar energy is used, not fossil fuel-based energy. Therefore, in addition to being sustainable, it creates a clean / emission-free hydrogen production potential.

Thermochemical cycle-based methods offer a solution to the simultaneous H_2 and O_2 production experienced in the thermolysis method. In two-step thermochemical cycles the release of H_2 and O_2 occurs at different stages and temperatures [8]. Therefore, pure hydrogen production can be achieved without the need for any separation process. Hydrogen production by thermochemical cycles occurs at very low temperatures (<1000 ° C) compared to thermolysis (Steinfeld, 2005). In addition, with thermochemical water splitting (TWS), which takes place in two-stage, hydrogen production can also benefit from the entire solar spectrum without any loss of natural resources [8], [9].

In the TWS method, the active materials where the reactions take place are typically oxygen-containing metal oxides (MO). Typical redox reactions occurring in TWS are shown as below;

1st step: MO_x (s) → $MO_{x-\delta}$ (s) + $\delta/2$ O_2 (g) (>1400°C)

2nd step: $MO_{x-\delta}$ (s) + δ H_2O (g) → MO_x (s) + δ H_2 (g) <1000 °C

In the first step, the reduction of the MO material with the energy it has received (solar energy) occurs. By reducing MO, oxygen vacancies are formed and O_2 release occurs at higher temperatures (T_{red}> 1400 °C) in the structure according to the metal oxide used. As a result of these reactions, O_2 is released. In the 2nd step, in which the oxidation reaction takes place, takes place at relatively lower temperatures (T_{ox} <1000 ° C), the reduced MO material reacts with the H_2O vapor in the environment, hydrogen production is provided. The metal oxide used in TWS provides oxygen transport in two-step redox reactions. For these reaction cycles to be sustainable, the metal oxide must be structurally and thermally stable [10]–[12]. Since it also affects the hydrogen production efficiency [10], [13], [14].

Perovskite oxide structures take attention with an allowance of non-stoichiometric oxygen amount [15]. It has been found that many perovskite oxides allow a high degree of non-stoichiometric oxygen while maintaining structural stability [16]–[18].

The most studied perovskite family for hydrogen production by TWS is the $LaMnO_3$ family because it offers higher structural stability compared to other perovskite oxides, has studies containing additive elements such as Sr, Ca and Ba used as doping elements to substitute La site. Among the studies, $LaMnO_3$ with Sr doping constitutes the most striking compositions [18], [19] whereas Ca using instead of Sr cause less distortion in the structure [20]. On the other hand, there are other studies that focus on the substitution of Al element to substitute Mn site due to its influence on structural stability [21].

As it is mentioned above, there is huge composition diversity for perovskite oxides and its structural, as well as morphological properties, are strongly affected by the variety of chemical compositions. Therefore, in the focus of those findings, the aim of this study to determine the effects of synthesis parameters on the structural and morphological properties of $La_{0.4}Ca_{0.6}Mn_{0.6}Al_{0.4}O_3$, and $La_{0.2}Ca_{0.8}Mn_{0.8}Al_{0.2}O_3$ perovskite-type oxides.

2. Experimental Procedure

In this study, $La_{0.4}Ca_{0.6}Mn_{0.6}Al_{0.4}O_3$ (LCMA4664), and $La_{0.2}Ca_{0.8}Mn_{0.8}Al_{0.2}O_3$ (LCMA2882) were synthesized by the Pechini method, which is a solution-based method

[22]. As precursors, $La(NO_3)_2.6H_2O$ (Alfa Aesar 99.99%), $Ca(NO_3)_2.4H_2O$ (Alfa Aesar 99.98%), $Mn(NO_3)_2.4H_2O$ (Merck ≥99%), and $Al(NO_3)_3.9H_2O$ (Carlo Erba ≥99%) were used as nitrate salts of metal cations (TM). Citric acid (CA) was added as a chelating agent with the ratio of TM:CA=1.00:1.50, whereas ethylene glycol (EG) was used as a polymerization agent. In the synthesis studies, comparative studies were carried out to regulate the pH value (pH = 8) and set as free (pH≤1.00) to examine the effect of pH as well as the effect of EG addition. To determine the effect of synthesis parameters; four different experimental conditions were assigned, as seen in Table 1.

Table 1. Four different experiment conditions were employed in the study.

#1	TM:CA=1.00:1.50, EG=0, no-pH control
#2	TM:CA=1.00:1.50 EG=0, pH=8.00
#3	TM:CA=1.00:1.50, EG=1.50, no-pH control
#4	TM:CA=1.00:1.50 EG=1.50, pH=8.00

Powders synthesized were dried in the drying oven at 250°C for 2 hours to remove residual organic components and salts, then calcined at 1300 °C for 6 hours to obtain a crystalline perovskite structure. In preliminary studies, calcination temperature was studied starting from 900°C and decided as 1300 °C where the most stable form, cubic, of perovskite, obtained without any secondary phases and no/small amount of other structural forms of perovskite with sufficient time to obtain desired crystal structure with smaller initial particle size.

X-Ray diffractometer (XRD, Rigaku Smartlab) using Bragg-Brentano geometry was performed with Cu-Kα (1.5406 Å) radiation to determine crystal structures and purity. The XRD patterns were collected over a scattering angle range between 10 and 90° using scan rate of 2°/min. In the existence of secondary phases, the amount of the phases was calculated using NIMS_MatNavi_4295518592_1_2 and NIMS_MatNavi_4296371477_1_2 crystallographic information file card for cubic and orthorhombic structure, respectively using Rietveld analysis software (MAUD ver. 2.79). The morphology of perovskite oxides and elemental analysis were examined by scanning electron microscopy (SEM, Jeol SM-7600F) using 20 kV accelerating voltage. In addition to these, the Brunauer-Emmett-Teller (BET) method was used to determine the surface area of the powders synthesized, and the analyzes were carried out in a single-pointed Quantachrome brand Autosorb-6B model surface adsorption device. Before the BET measurements, the powders were heated at 300 °C for 5 hours in order to remove the external gases inside the powders. Surface measurements using nitrogen gas for adsorption typically took 1 hour.

3. Results and Discussion

XRD was performed to analyze the phases of the powders synthesized and calcined. The XRD patterns obtained are given in Figure 1. It is seen that the LCMA dominant structure is cubic for all conditions. However, it was determined that some orthorhombic LCMA was formed in both pH conditions (7.70% and 1.60% by weight) where there was no EG addition. This situation was also confirmed in the Rietveld analysis. Table 2. X-ray diffraction of the orthorhombic crystal structure was not found in cases involving EG addition.

Table 2. Rietveld analysis results of XRD patterns obtained after 6 hours calcination process of LCMA4664 powders synthesized under different conditions.

	wt. %	
Sample	**Cubic LCMA**	**Orthorhombic LCMA**
LCMA4664-1300-6	92.30	7.70
LCMA4664-pH-1300-6	98.40	1.60
LCMA4664-EG-1300-6	100.00	-
LCMA4664-EG-pH-1300-6	100.00	-
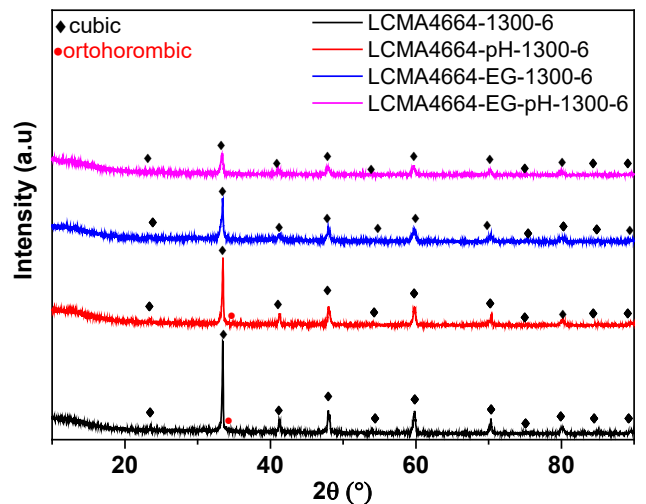
Figure 1. XRD analysis of LCMA4664 powders synthesized under four different conditions after calcining at 1300 ° C for 6 hours. The diffraction angles of the cubic LCMA phase are indicated by the symbol • and the orthorhombic LCMA phase by the symbol. *In the figure, only the diffractions of the orthorhombic phase that do not overlap with the cubic phase are indicated in order to avoid confusion.*

Subsequently, the powders produced were analyzed to examine the surface morphology and to determine the chemical composition by SEM, Figure 2, and EDS, Table 3, respectively. With the margin of error (~2%) of the EDS analysis [12,13], it is seen that the composition

values obtained from the synthesis were at an acceptable level where the expected stoichiometric distribution for the LCMA4664 composition was atomically La = 20%, Ca = 30%, Mn = 30% and Al = 20%.

Table 3. EDS analysis results of LCMA4664 powders synthesized under different conditions and calcined at 1300 °C for 6 hours.

Sample	at. %			
	La	**Ca**	**Mn**	**Al**
LCMA4664-1300-6	20.15	29.63	29.99	20.23
LCMA4664-pH-1300-6	21.06	29.55	28.95	20.44
LCMA4664-EG-1300-6	20.98	29.04	28.34	21.64
LCMA4664-EG-pH-1300-6	21.20	29.09	29.61	20.10

SEM studies showed that a similar grain structure was formed in LCMA4664 compositions produced under different synthesis conditions. It was seen that all powders obtained under different synthesis conditions suffering from sintering after the calcination at 1300 °C. This observation is quite consistent with the known sintering problem of LCMA [19]. SEM investigations showed that particles of LCMA4664 compositions were approximately with a size range of 50nm and coarse grains mainly 500nm.
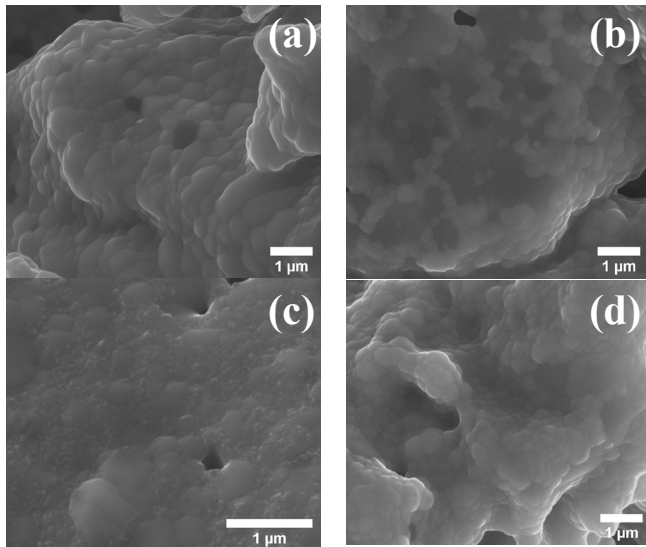

Figure 2. (a) LCMA4664-1300-6, (b) LCMA4664-pH-1300-6, (c) LCMA4664-EG-1300-6, and (d), LCMA4664-EG-pH-1300-6 SEM images of LCMA powders.

Powders were analyzed by BET method in order to measure precisely the surface areas of powders obtained under different synthesis conditions, Table 4. Consistent with the sintering problem detected in SEM images, very low surface area, in the range of 0.36-1.23 m^2/g, were measured in LCMA4664 powders belong to different syntheses.

Table 4. BET analysis results of LCMA4664 powders synthesized under different conditions and calcined at 1300 °C for 6 hours.

Sample	Surface area (m^2/g)
LCMA4664-1300-6	0.69
LCMA4664-pH-1300-6	0.81
LCMA4664-EG-1300-6	0.36
LCMA4664-EG-pH-1300-6	1.23

The same synthesis procedure was applied to LCMA2882 perovskite oxides having different stoichiometric ratio with increasing amount of Ca. The aim here was to compare the results of the synthesis conditions for also LCMA2882 compositions. The powders produced were primarily analyzed by XRD, thus phase purity was confirmed. Relevant XRD patterns are given in Figure 3.
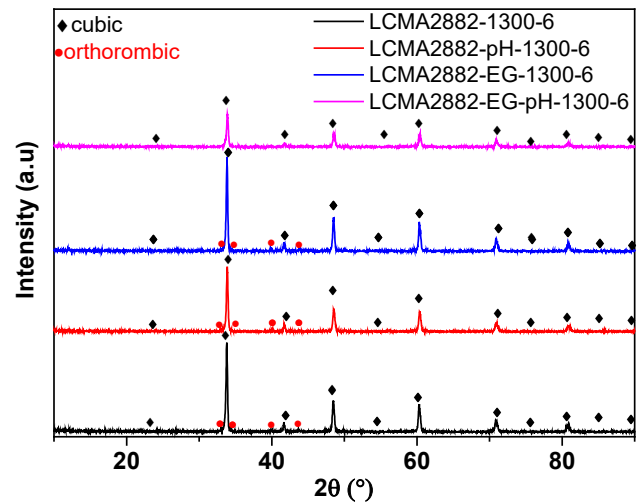
Figure 3. XRD analysis of LCMA2882 powders synthesized under four different conditions after calcining at 1300 °C for 6 hours. The diffraction angles of the cubic LCMA phase are indicated by the symbol • and the orthorhombic LCMA phase by the symbol. *In the figure, only the diffractions of the orthorhombic phase that do not overlap with the cubic phase are indicated to prevent confusion.*

XRD analyses showed that the single-phase cubic LCMA2882 structure was formed with synthesis parameters using only EG and providing the pH = 8.00 condition. No orthorhombic X-ray diffraction could be detected for this synthesis parameter under XRD analysis conditions. Although cubic structure was obtained principally in other synthesis conditions, orthorhombic LCMA formation was detected with higher weight percentage. This has been confirmed by Rietveld analyses, Table 5.

Table 5. Rietveld analysis results of XRD patterns obtained after 6 hours of calcination at 1300 °C of

LCMA2882 powders synthesized under different conditions.

Sample	wt. %	
	Cubic LCMA	Orthorhombic LCMA
LCMA2882-1300-6	32.00	68.00
LCMA2882-pH-1300-6	30.50	69.50
LCMA2882-EG-1300-6	12.00	88.00
LCMA2882-EG-pH-1300-6	100.00	-

The powders produced were analyzed to examine the surface morphology and to determine the chemical composition by SEM, Figure4, and EDS, Table 4, respectively. It was observed that the composition values obtained from the synthesis are at an acceptable level where the expected stoichiometric distribution for the LCMA2882 composition was atomically La = 10%, Ca = 40%, Mn = 40% and Al = 10%.
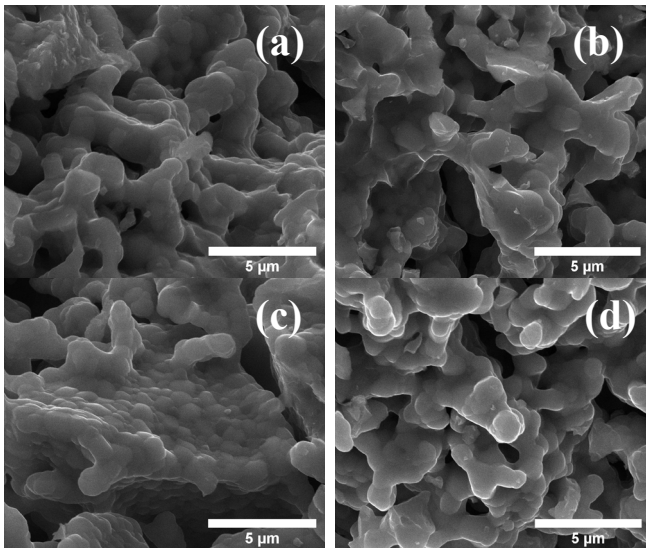
Figure 4. (a) LCMA2882-1300-6, (b) LCMA2882-pH-1300-6, (c) LCMA2882-EG-1300-6, and (d), LCMA2882-EG-pH-1300-6 SEM images of LCMA powders.

Table 6. EDS analysis results of LCMA2882 powders synthesized under different conditions and calcined at 1300 °C for 6 hours.

Sample	at. %			
	La	Ca	Mn	Al
LCMA2882-1300-6	10.93	40.83	38:98	9.26
LCMA2882-pH-1300-6	10.69	40.07	38.59	10.65
LCMA2882-EG-1300-6	10.96	40.40	39.29	9.50
LCMA2882-EG-pH-1300-6	10.24	40.69	39.78	9.29

SEM investigation of LCMA2882 compositions showed that there was an occurrence of coarsening of the particle size with a more porous structure. However, the determined surface area is still smaller which is in the range of 0.87-2.64 m²/g, Table 7, compared to other perovskite oxide compositions [23], [24].

Table 7. BET analysis results of LCMA2882 powders synthesized under different conditions and calcined at 1300 °C for 6 hours.

Sample	Surface area (m²/g)
LCMA2882-1300-6	0.87
LCMA2882-pH-1300-6	0.96
LCMA2882-EG-1300-6	0.97
LCMA2882-EG-pH-1300-6	2.64

4. Conclusion

In this study, La$_{1-x}$Ca$_x$Mn$_y$Al$_{1-y}$ perovskites were synthesized by Pechini method. To understand structural stability of the compositions, the different stoichiometric ratio of the compositions was synthesized under the same conditions. It was found that LCMA2882 composition tends to transform into the orthorhombic structure almost for all synthesis conditions except the addition of EG and pH-controlled whereas LCMA4664 perovskite oxide was an almost cubic structure for all synthesis conditions. It can be commented on that the morphology of perovskite was slightly affected by changing the amount of composition. Since it was observed that LCMA2882 compositions have a more porous structure with larger final particles than that of LCMA4664 perovskite oxide. Moreover, all the samples of LCMA2882 have higher surface area than the same counterparts of LCMA4664 which may be due to having a two-phase structure. Consequently, both perovskite oxides, LCMA4664 and LCMA2882, seem suitable candidates for two-step thermochemical water splitting reactions that can be tested for hydrogen production.

5. References

[1] U. Bossel and B. Eliasson, "Energy and the Hydrogen Economy," *ABB Switz. Ltd*, pp. 1–35, 2009.

[2] J. M. Ogden, "Prospects for Building a Hydrogen Energy Infrastructure," *Annu. Rev. Energy Environ.*, vol. 24, no. 1, pp. 227–279, 1999.

[3] L. Ager-Wick Ellingsen *et al.*, "Nanotechnology for environmentally sustainable electromobility Life-cycle assessment of EVs," *Nat. Publ. Gr.*, vol. 11, no. 12, pp. 1039–1051, 2016.

[4] T. M. Nenoff, R. J. Spontak, and C. M. Aberg, "Membranes for Hydrogen Purification: An Important Step toward a Hydrogen-Based Economy," *MRS Bull.*, vol. 31, no. 10, pp. 735–744, 2006.

[5] J. G. Xu and G. F. Froment, "Methane Steam Reforming, Methanation and Water-Gas Shift .1.

Intrinsic Kinetics," *Aiche J.*, vol. 35, no. 1, pp. 88–96, 1989.

[6] N. S. Lewis and D. G. Nocera, "Powering the planet: Chemical challenges in solar energy utilization," *Proc. Natl. Acad. Sci.*, vol. 103, no. 43, pp. 15729 LP – 15735, 2006.

[7] P. Nikolaidis and A. Poullikkas, "A comparative overview of hydrogen production processes," *Renew. Sustain. Energy Rev.*, vol. 67, pp. 597–611, 2017.

[8] N. P. Siegel, J. E. Miller, I. Ermanoski, R. B. Diver, and E. B. Stechel, "Factors Affecting the Efficiency of Solar Driven Metal Oxide Thermochemical Cycles," *Ind. Eng. Chem. Res.*, vol. 52, no. 9, pp. 3276–3286, 2013.

[9] M. Roeb *et al.*, "Materials-Related Aspects of Thermochemical Water and Carbon Dioxide Splitting: A Review," *Materials (Basel).*, vol. 5, no. 11, pp. 2015–2054, 2012.

[10] J. R. Scheffe and A. Steinfeld, "Oxygen exchange materials for solar thermochemical splitting of H2O and CO2: a review," *Mater. Today*, vol. 17, no. 7, pp. 341–348, 2014.

[11] Z. Zhao, M. Uddi, N. Tsvetkov, B. Yildiz, and A. F. Ghoniem, "Redox Kinetics Study of Fuel Reduced Ceria for Chemical-Looping Water Splitting," *J. Phys. Chem. C*, vol. 120, no. 30, pp. 16271–16289, 2016.

[12] Y. Sugiyama, N. Gokon, H. Cho, S. Bellan, and T. Hatamachi, "Thermochemical Two-Step Water-Splitting Using Perovskite," pp. 1–6, 2017.

[13] A. Steinfeld, "Solar hydrogen production via a two-step water-splitting thermochemical cycle based on Zn/ZnO redox reactions," *Int. J. Hydrogen Energy*, vol. 27, no. 6, pp. 611–619, 2002.

[14] A. A. Emery, J. E. Saal, S. Kirklin, V. I. Hegde, and C. Wolverton, "High-Throughput Computational Screening of Perovskites for Thermochemical Water Splitting Applications," *Chem. Mater.*, vol. 28, no. 16, pp. 5621–5634, 2016.

[15] C. N. R. Rao and S. Dey, "Solar thermochemical splitting of water to generate hydrogen," *Proc. Natl. Acad. Sci.*, vol. 2017, p. 201700104, 2017.

[16] A. H. McDaniel *et al.*, "Nonstoichiometric perovskite oxides for solar thermochemical H2 and CO production," *Energy Procedia*, vol. 49, no. December 2014, pp. 2009–2018, 2013.

[17] J. E. Miller, A. Ambrosini, E. N. Coker, M. D. Allendorf, and A. H. McDaniel, "Advancing oxide materials for thermochemical production of solar fuels," *Energy Procedia*, vol. 49, pp. 2019–2026, 2013.

[18] J. R. Scheffe, D. Weibel, and A. Steinfeld, "Lanthanum-strontium-manganese perovskites as redox materials for solar thermochemical splitting of H2O and CO2," in *Energy and Fuels*, 2013.

[19] C.-K. Yang, Y. Yamazaki, A. Aydin, and S. M. Haile, "Thermodynamic and kinetic assessments of strontium-doped lanthanum manganite perovskites for two-step thermochemical water splitting," *J. Mater. Chem. A*, vol. 2, no. 33, pp. 13612–13623, 2014.

[20] A. Demont and S. Abanades, "Solar thermochemical conversion of CO2 into fuel via two-step redox cycling of non-stoichiometric Mn-containing perovskite oxides," *J. Mater. Chem. A*, 2015.

[21] D. Sastre, A. J. Carrillo, D. P. Serrano, P. Pizarro, and J. M. Coronado, "Exploring the Redox Behavior of La0.6Sr0.4Mn1−xAlxO3 Perovskites for CO2-Splitting in Thermochemical Cycles," *Top. Catal.*, vol. 60, no. 15–16, pp. 1108–1118, Sep. 2017.

[22] M. P. Pechini, "Method of preparing lead and alkaline earth titanates and niobates and coating method using the same to form a capacitor." US Patent Office, 1967.

[23] A. M. Kamarul Bahrain, S. Ida, and T. Ishihara, "Al-doped La0.5Sr0.5MnO3 as oxide anode for solid oxide fuel cells using dry C3H8 fuel," *J. Solid State Electrochem.*, vol. 21, no. 1, pp. 161–170, 2017.

[24] L. Wang *et al.*, "Ca $^{2+}$ and Ga $^{3+}$ doped LaMnO $_3$ perovskite as a highly efficient and stable catalyst for two-step thermochemical water splitting," *Sustain. Energy Fuels*, vol. 1, no. 5, pp. 1013–1017, 2017.